Landscape- and site-scale spatial variability of blue carbon stocks and fluxes in tropical seagrass meadows

Naima Iram[1]*, Kiah Eng Lim[2], Muhammad Ariq Khalingga[1], Pierre Taillardat,[3] Sheryl Chan Si Ern[1], Lian Pin Koh[1]*, Daniel A. Friess[4]

[1]Centre for Nature-based Climate Solutions, Department of Biological Sciences, National University of Singapore, Singapore, 117558, Singapore
[2]Department of Biological Sciences, National University of Singapore, Singapore, 117558, Singapore
[3]Asian School of the Environment, Nanyang Technological University, Singapore, Singapore
[4]Department of Earth and Environmental Sciences, Tulane University, New Orleans, 70118, USA

*Correspondence to: Naima Iram (n.iram@nus.edu.sg), Lian Pin Koh (lianpinkoh@nus.edu.sg)

Abstract. Seagrass meadows are emerging natural climate solutions for climate change mitigation through their high potential for organic carbon sequestration and storage, also known as blue carbon. However, the variability in current blue carbon stock and flux estimates is high, particularly at landscape scales. This knowledge gap highlights the need for evaluating blue carbon at spatial scales that are both locally robust and globally relevant. We quantified the magnitude of variability in blue carbon stocks and fluxes in tropical intertidal seagrass meadows at the site and landscape scales. We sampled within and across six intertidal seagrass meadows representing three geomorphic settings, including reef-associated settings dominated by *Cymodocea* spp., estuaries *Halophila* spp. and lagoons~~,~~ dominated by *Thalassia* spp., across Singapore. Within and a~~A~~cross these sites, we measured soil organic carbon (C_{org}) stocks and greenhouse gas fluxes using the static chamber method. ~~We found that~~ T~~t~~ropical intertidal seagrass meadows stored ~~132 ± 78 Mg C_{org} ha^{-1} (mean ± SD) in the top 100 cm of soil, which varied significantly within sites and geomorphic settings (min–max: 19–303 Mg C_{org} ha^{-1}), and were positively associated with salinity. Seagrass fluxes averaged 660 ± 695 mg m^{-2} d^{-1} of CO_2 and 12 ± 484 µg m^{-2} d^{-1} of CH4, which, unlike stocks, did not appear to vary significantly across geomorphic settings. However, we identified redox (positive) and bulk density (negative) as independent drivers of CO_2, and C_{org} as an independent, strong predictor of CH_4 after accounting for spatial hierarchy and geomorphic setting. Spatially explicit stock assessments and inclusion of greenhouse gas fluxes are important to inform robust coastal carbon budgeting and support the inclusion of seagrass in national climate mitigation frameworks.~~ 27.5 ± 19.9 Mg C_{org} ha^{-1} (mean ± SD) in the top 0-25 cm of soil, which varied significantly within sites (min-max: 5.1-78.9 Mg C_{org} ha^{-1}, n=42). Plot-level mean fluxes averaged 27.5 ± 25.3 mg m^{-2} h^{-1} of CO_2 (min–max: −18.6 to 82.4, n=54) and 0.5 ± 18.2 µg m^{-2} h^{-1} of CH_4 (min–max: −66.4 to 57.5, n=56). Mixed-effects models indicated that geomorphic setting did not explain variation in 0–25 cm stocks or in CO_2 and CH_4 fluxes. Sensitivity analyses for 0–100 cm stocks showed a marginal geomorphology effect for measured-only totals (p = 0.074) that was not present after extrapolation to 100 cm (p = 0.816). In multivariate driver models, CO_2 flux was negatively associated with water temperature (p = 0.011) and showed an overall geomorphology effect (p = 0.027), while CH_4 drivers were not resolved (all $p \geq 0.158$. Plot-level modelling further showed that CO_2 decreased with

Formatted: Not Highlight

increasing 0–25 cm stock (p = 0.044), whereas CH_4 showed no association with stock (p = 0.469). Overall, these results highlight strong spatial heterogeneity in tropical intertidal seagrass carbon dynamics and underscore the need for spatially explicit sampling and modelling frameworks that reflect nested spatial structure.

1 Introduction

Seagrass meadows have a high capacity for storing organic carbon, in their sediments and are widely recognised as blue carbon ecosystems, where conservation and restoration are used to protect and enhance these sediment carbon stocks as a nature-based solutions to climate-change mitigation also known as blue carbon, and are therefore widely recognised as emerging natural climate solutions for climate change mitigation (Unsworth et al., 2022; Duarte et al., 2025; Do Amaral Camara Lima et al., 2023). Yet seagrasses globally face a high risk of degradation, which could lead to ~ 1,154 Tg CO_2 emissions with a social cost of $213 billion USD (Krause et al., 2025b). Therefore, there is a global interest in incorporating the conservation and restoration of seagrass meadows into climate change mitigation schemes and policies, such as a country's Nationally Determined Contribution (NDC) to the Paris Agreement and associated Nationally Appropriate Mitigation Actions (NAMAs) (Macreadie et al., 2021). However, policies and management decisions should be guided by a robust evidence base, including credible estimates of the extent, drivers and patterns of organic carbon storage (Dahl et al., 2025).

Although knowledge and understanding of the magnitude and drivers of variation in organic carbon (C_{org}) storage in seagrass meadows has greatly increased recently at the global scale (Gomis et al., 2025; Krause et al., 2025b), there are still challenges in quantifying blue carbon at site-specific or landscape scales, which is a mosaic of habitats with unique essentially an ecosystem and its surrounding biophysical environment, hindering global efforts to establish them as reliable natural climate solutions (Williamson et al., 2022; Stankovic et al., 2023). Variability in seagrass C_{org} and carbon budgets is driven by biotic and abiotic factors at various spatial scales (Krause et al., 2025b; Gomis et al., 2025; Mazarrasa et al., 2021; Mazarrasa et al., 2023). At the intra-site scale, extrapolating standard 100 cm C_{org} stocks from shallower cores is a major caveat, potentially leading to 1.5- to 10-fold overunderestimation (Dahl et al., 2025; Stankovic et al., 2023; Krause et al., 2025b). Local or site-scale variability of C_{org} is generally attributed to grain size (Miyajima et al., 2015), species composition (Gomis et al., 2025), the contribution of sources of organic matter, i.e. autochthonous and allochthonous (Ricart et al., 2020; Serrano et al., 2019), water depth, and hydrodynamic energy, etc. (Lavery et al., 2013; Ndhlovu et al., 2024; York et al., 2018). However, our understanding of how these factors scale to broader landscape contexts remains incomplete.

At larger landscape scales, the coastal geomorphic setting has emerged as a key control on seagrass C_{org} variability (Kennedy et al., 2022; Mazarrasa et al., 2021); however, it is not known how the geomorphic setting would influence GHG emissions from seagrasses. Estuarine meadows generally inhabit the intertidal interface and shallower depths, receive large inputs of terrigenous organic material, and experience low hydrodynamic energy, creating a depositional environment (Ricart et al., 2020), potentially facilitating high accumulation of allochthonous carbon (Capece et al., 2025). Sheltered coastal settings—

such as lagoons or back-reef meadows—can maintain higher surface-soil C_{org} due to reduced sediment resuspension and wave energy (Guerra-Vargas et al., 2020; Alemu et al., 2022). However, typical anoxic conditions and high organic matter inputs in seagrasses that promote high C_{org} burial and sequestration can also favour the production and emission of greenhouse gases such as methane (CH_4) (Rosentreter et al., 2021). Seagrass meadows appear to be negligible to moderate CH_4 sources, ranging from 0.3 to 378 µg m^{-2} h^{-1} and potentially offsetting ~12–78 times the CO_2 equivalents of their carbon accumulation rates (Asplund et al., 2022; Burkholz et al., 2020). However, the ecosystem will ultimately produce a negative net radiative balance over sufficiently long-time scales because CH_4 has a much shorter atmospheric lifetime than CO_2 ((Neubauer and Megonigal, 2015)).Thus, geomorphic environmental gradients are expected to affect GHG emissions such that GHG emissions could be elevated in estuarine or sheltered seagrass meadows where C_{org} stocks are potentially higher. Kirwan et al. (2023) proposed that GHG emissions in coastal wetlands would be governed by local-scale factors plant productivity and electron acceptor availability compared to landscape-scale geomorphic processes, yet this hypothesis has not been explicitly tested across geomorphic settings in seagrass meadows.

Here, we explore the spatial variability in carbon stocks and fluxes across seagrass meadows of different geomorphic settings in Singapore. We hypothesised that geomorphic settings such as reef-associated settings, estuaries and lagoonal settings would shape soil organic carbon and GHG emissions in tropical seagrass meadows, and a higher soil C_{org} would be associated with higher GHG fluxes under these geomorphic ~~gradients~~ types. Here, we use 'landscape scale' to refer to a mosaic of seagrass meadows distributed across different geomorphic settings (reef-associated, lagoonal, and estuarine) within Singapore, where larger-scale drivers of stocks and fluxes such as temperature and precipitation are held constant. We ask 1) what is the magnitude of soil organic carbon stocks and GHG emissions (CO_2 and CH_4) of tropical seagrass meadows, 2) How do organic carbon and GHG fluxes vary across spatial scales encompassing local (within-site, across sites) and landscape (geomorphic settings) levels, and 3) are patterns in organic carbon storage associated with GHG fluxes, and which environmental parameters define these associations?

2 Methodology

2.1 Site description

The study was conducted on six intertidal seagrass meadows across the tropical island state of Singapore (Fig. 1). The climate of the area is humid tropical; therefore, temperature does not vary much throughout the year, with the highest average monthly temperature of 28.8°C during May and the lowest average monthly temperature of 26.8°C during December and January (Meteorological Service Singapore, 2024). Mean annual rainfall is 2,113 mm (1991–2024), with two monsoon periods during June–September and December–early March separated by inter-monsoon seasons in late March–May and October–November. The seagrass meadows in this study are found in the lower intertidal zone and experience a diurnal tidal cycle, such that they are only briefly exposed during low tide (<0.7m, tidal range >2.5 m) and remain fully submerged during high tide. ~~These~~

meadows experience a diurnal tidal cycle such that they are only briefly exposed during low tide (<0.7m, tidal range >2.5 m) and remain fully submerged during high tide. We selected six intertidal meadows representing three geomorphic classes (Mckenzie et al., 2016): reef-associated (Cyrene Reef, Labrador Nature Reserve; dominated by *Cymodocea* spp.), lagoonal (Tanah Merah, Eagle Bay; dominated by *Thalassia* spp.), and estuarine (Chek Jawa, Changi Beach Park, dominated by *Halophila* spp., Fig. 1). Supplement Table S1 summarises seagrass species composition and cover by site.

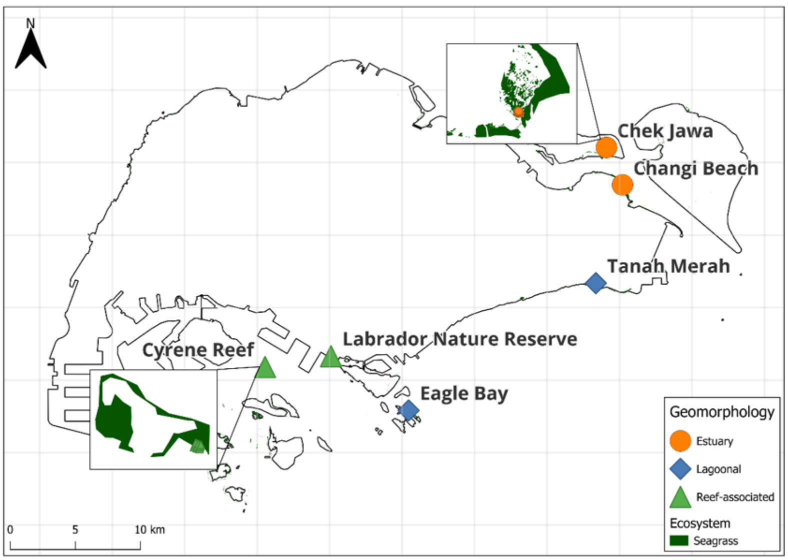

Figure 1. Extent of seagrass across Singapore (Tan et al., 2022) and study sites locations of intertidal seagrass meadows across estuarine, lagoonal and reef-associated geomorphic settings. Two sites with the largest seagrass extent among the studied sites are zoomed in.

Formatted: Keep with next

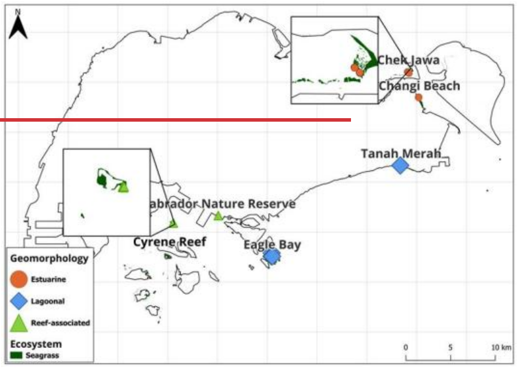

~~**Figure 1: Singapore seagrass extent map (Tan et al., 2022) and study sites locations of intertidal seagrass meadows across estuarine, lagoonal and reef-associated geomorphic settings. Two sites with the largest seagrass extent among the studied sites are zoomed in.**~~

2.2 Field sampling design

We collected field data during low tide from October 2022 to May 2024 and targeted the same time of the day and season for consistency and to avoid seasonal variations affecting GHG fluxes. We selected the sampling months when Singapore's climate is generally consistent with an average monthly temperature of 27.5-28.8°C and average monthly rainfall of 150-160 mm (Meteorological Service Singapore, 2024). At each site, 3–5 transects (30 m length treated as within-site sampling units) were laid parallel to shore at approximately similar tidal exposure and elevations, >5 m apart, positioned to encompass the meadow extent following visual assessment. Three 1 m × 1 m plots were established along each transect at 5, 15, and 25 m. Where transects could not capture site heterogeneity, additional random plots were sampled within the meadow to improve coverage.

2.3 Carbon stocks

To quantify sediment carbon stocks, we collected 9–15 replicate sediment cores per site using a gouge auger (5.08 cm internal diameter) to 1 m depth or refusal. Because the upper 20–50 cm typically exhibits the strongest gradients in carbon content ((Howard, 2014)~~ref~~) due to the influence of the vegetation rooting zone, the top 50 cm was sectioned at 5 cm increments. Each core was divided into 11 sections: 0–5, 5–10, 10–15, 15–20, 20–25, 25–30, 30–35, 35–40, 40–45, 45–50, and 50–100 cm. We used 5 cm increments in the upper 50 cm to capture steep near-surface gradients commonly observed in seagrass sediments (Howard et al., 2014). Below 50 cm, we used a coarser interval (50–100 cm) due to expected lower variation in carbon stocks at depth (Phang et al., 2015). Core compaction during extraction was minimal (<10%). Sediment was transported to the laboratory and dried at 60 °C to a constant mass. Dry bulk density (g dry weight cm^{-3}) was calculated as dry mass divided by the in-situ sample volume (Howard et al., 2014). A subsample was ground and homogenised, then fumigated overnight with

Formatted: Superscript

0.1 M HCl to remove inorganic carbon, dried, weighed, encapsulated in tin, and analysed for total organic carbon (C_{org}, %) using an organic carbon analyser. Carbon stocks (Mg C_{org} ha^{-1}) were calculated following Howard et al. (2014), integrating section-specific C_{org}, dry bulk density, and layer thickness. ~~to 1 m (or core maximum) and upscaling to a hectare. Shorter cores were extrapolated linearly up to 1 m, and carbon stocks were reported at 15cm, 30 cm and 1 m depth for comparison (Table 1).~~ We recorded core refusal depth (cm) during sampling and treated refusal depth as an informative sediment property reflecting sediment deposit thickness. Of the 62 cores collected, 25 (40.3%) reached 100 cm depth, and 25 (40.3%) reached ≥80 cm depth (based on refusal depth). Our primary carbon stock response was measured only soil organic carbon stock in the 0–25 cm interval. To ensure comparable depth coverage across sites, primary inference for 0–25 cm stocks was restricted to cores that reached ≥25 cm depth ("complete-to-25" cores; n=42). We report 0–100 cm stocks as secondary sensitivity estimates (measured-only and extrapolated-to-100 cm), clearly labelled. For cores shorter than 100 cm, we extrapolated linearly from the deepest measured interval to 100 cm. For sediment texture ~~grain size~~, dried subsamples were disaggregated, sieved at 2 mm to remove coarse fragments (shells, pebbles), dispersed in deionised water, and analysed with a laser diffraction particle size analyser (Horiba LA, 350). Sediment texture was characterised using the mud fraction (% mud) measured for each depth interval; for modelling we summarised mud fraction as the mean % mud within 0–25 cm at the core level (stock models) and at the plot level (flux driver models).
~~, reporting median grain size (µm).~~

2.4 Sediment-air greenhouse gas fluxes

We used opaque (dark) static chambers to quantify s~~S~~ediment–air CO_2 and CH_4 fluxes ~~were measured~~ during low tide exposure representing representing sediment respiration/production, rather than net ecosystem exchange that would include photosynthetic uptake. Chamber collars (PVC, internal diameter 15 cm) were inserted ~5 cm into the sediment. We minimised disturbance by careful insertion and waiting for a 20-minute equilibration period before T_0 sampling based on our observations from a previous study ((Iram et al., 2022)). Chambers were rigid PVC with an enclosed headspace height of 30 cm. Lids were sealed using rubber bands and inspected sealing surface carefully to rule out leaks. Measurements were conducted once for each site between 10:00 and 17:00 to minimise diel variability. ~~using static, manual dark chambers. Chambers consisted of round PVC collars (internal diameter 15 cm) inserted 5 cm into the sediment, fitted with airtight lids; total enclosed headspace height was 30 cm.~~ Within each plot, three chambers were deployed at random positions and sealed ~~(~~with rubber bands~~/gaskets).~~ Headspace gas was sampled by syringe at 0, 20, 40, and 60 min and transferred to 15mL pre-evacuated glass vials (Labco, High Wycombe, UK). Concentrations were measured in the laboratory using a cavity ring-down spectrometer (Picarro G220-i). Fluxes (surface-area-normalised) were calculated from the linear rate of change in headspace concentration over time, corrected for chamber volume, surface area, ambient temperature and pressure via the ideal gas law. Flux estimates were retained when linear fits met $r^2 \geq 0.8$ (162/180) and non-linear estimates were excluded.

2.5 Environmental parameters

At each plot, we measured surface sediment temperature (°C) at the top 5 cm depth using an Electronic 4-in-1 soil meter. Sediment redox potential (mV), pH, salinity (psu), surface water temperature (°C), conductivity (mS/cm) and dissolved oxygen (%) were measured using a multiparameter Hanna® pH/ORP sensor (HI769819X) immediately adjacent to chambers during low tide, allowing readings to stabilise for 5 minutes. Air temperature (°C) inside each chamber was measured using a Hobo® Pendant MX Tem. All sensors were calibrated following the manufacturer's guidelines before each field campaign.

2..65 Data Analysis

~~Data were tested for normality through the Kolmogorov–Smirnov and Shapiro–Wilk tests. When data did not comply with the requirements of normality and homoscedasticity, we performed log, inverse, or square root transformations to meet the assumptions of normality. For data that was not normal after transformations, we performed a Kruskal–Wallis test followed by Dunn's test with Bonferroni correction to assess the significance of differences among plots, sites and geomorphic settings. We quantified monotonic associations among environmental variables, soil carbon metrics, and fluxes using pairwise Spearman rank correlations. With 15 variables, there were 105 unique pairs. To control for multiple testing across all pairs, p-values were adjusted using the Benjamini–Hochberg FDR procedure (reporting q-values). We identified near-duplicate (redundant) predictors as those with |ρ| ≥ 0.95 (e.g., pH vs redox; salinity vs conductivity; water vs soil temperature) and included a single representative from each redundant pair for interpretation and modelling. To examine the hierarchical variance in greenhouse gas fluxes and their relationship with environmental parameters, we used mixed-effect models with random intercepts for plots nested within transects nested within sites and included geomorphic setting as a fixed effect. Model performance was assessed using marginal and conditional R2, AIC, and leave-one-site-out cross-validation. Model families and link functions were chosen based on response distributions: Gaussian for approximately normal responses (on transformed scales if needed), or Gamma with a log link for positive, right-skewed fluxes. Predictors were centred and scaled to aid interpretation and convergence. Analyses were run in R using the following packages: dunn.test or FSA for Dunn's tests, car for VIF, multcomp or emmeans for post-hoc contrasts, ggplot2 for figures. Spearman correlations and FDR adjustments used stats::cor.test and p.adjust(method = "BH").~~

All analyses were conducted in R (R Core Team, 2026) using lme4 (Bates et al., 2015) and lmerTest (Kuznetsova et al., 2017) for linear mixed-effects models (LMMs) and emmeans (Lenth and Piaskowski, 2026) for estimated marginal means. The primary stock response was 0–25 cm measured-only C_{org} stock restricted to 0-25 cm cores. Geomorphic setting effects on 0–25 cm stocks were tested using: $Stock_{0-25}$ ~ geomorphology + (1| site/transect).

Fluxes were analysed on the raw scale using Gaussian LMMs; negative fluxes were retained. CO_2 geomorphology-only models used plots nested within transects nested within sites (1| site/transect/plot). For CH_4, the fully nested model was singular; therefore, the geomorphology-only inference used a stable structure (1| site/plot). Fixed effects were tested using Type III tests with Satterthwaite denominator degrees of freedom (lmerTest).

To assess environmental controls on fluxes, we fit multivariate driver models including standardised (z-scored) predictors of redox, salinity, pH, water temperature, dissolved oxygen, and mud fraction (mean mud% in 0–25 cm), plus geomorphology. Conductivity was treated as redundant with salinity and was not included simultaneously. Pairwise comparisons among geomorphic classes and among sites were computed using Tukey-adjusted contrasts from estimated marginal means (emmeans); outputs are provided in the Supplement. We quantified how variability was distributed across spatial scales by extracting variance components from the fitted mixed models and expressing each component as a percentage of total variance (Supplement Table S2). We additionally explored an expanded within-site stock driver model including depth-resolved sediment properties (0–25 cm mud fraction and dry bulk density) and plot-level environmental covariates (salinity, redox, pH, temperature, dissolved oxygen), with predictors centred within site to separate within-site from between-site effects (Supplement Table S2). Supplement Table S2 provides full site-level variability outputs, including contrasts/EMMs with letters and N, refusal depth summaries, and variance partitioning.

Formatted: Font: (Default) +Body (Times New Roman)

2.76 Methodological limitations

We acknowledge the methodological limitations of our study due to logistical constraints. For this study, we targeted high-resolution spatial variation within the sites, including intensive replication of ≤ 15 soil cores and 27 chambers per site; however, for gas flux measurements, our study is limited to temporal replication of daily and seasonal changes First, while we targeted high-resolution spatial replication within sites (≤15 soil cores and 27 chambers per site), gas flux measurements are limited in temporal replication (e.g., diel/seasonal variability and high-tide conditions and tidal range variability among sites were not sampled). As such, we limit data reporting to per hr, not per day or per year. Second, below 50 cm depth we used a coarser core interval (50–100 cm) to prioritise replication, which may smooth fine-scale variability at depth and therefore interpretation of deep-layer estimates should be treated accordingly. However, based on prior measurements of seagrass meadows and other intertidal ecosystems in Singapore, we do not anticipate substantial variation in carbons stocks at lower depths (Phang et al., 2015). Third, chamber collars were inserted shortly before measurements due to access constraints during short low-tide windows; despite a 20-minute equilibration period, some disturbance effects may remain. Fourth, we acknowledge that low-tide dark-chamber fluxes may differ under high-tide inundation due to altered oxidation/transport conditions; however, in this study, we are interested in sediment-air fluxes, rather than sediment-water fluxes.

3 Results

3.1 Soil carbon stocks and fluxes in tropical seagrass meadows

We standardised soil organic carbon (C_{org}) stocks to 0–25 cm as the primary reporting depth because 25 cm was the maximum common measured depth across sites. Across all cores, 0–25 cm C_{org} stocks averaged 27.5 ± 19.9 Mg C_{org} ha^{-1} (mean ± SD;

range 5.1–78.9; n = 42 cores; Fig. 2). Seagrasses had plot-level mean CO_2 fluxes of 27.5 ± 25.7 mg m^{-2} h^{-1} (Range: -18.6 to 82.4 mg m^{-2} h^{-1}, n= 54 plots, Fig 3) and CH_4 fluxes of 0.5 ± 18.2 µg m^{-2} h^{-1} (Range: -66.4 to 57.5 µg m^{-2} h^{-1}, n = 54 plots; Fig. 4) for all measured sites.

Total organic carbon across seagrass ecosystems averaged 1.1 ± 0.8% (Range: 0.1 to 3.6%) for all study locations. Soil carbon stocks recorded in the top 100 cm of seagrass meadows were 131.6 ± 77.6 Mg ha^{-1} (Range: 18.8 to 302.6 Mg ha^{-1}). Seagrasses had CO_2 fluxes of 30.5 ± 27.8 mg m^{-2} h^{-1} (Range: -73.9 to 95 mg m^{-2} h^{-1}) and CH_4 fluxes of 0.8 ± 20.4 µg m^{-2} h^{-1} (Range: -76.5 to 81.8 µg m^{-2} h^{-1}) for all measured sites.

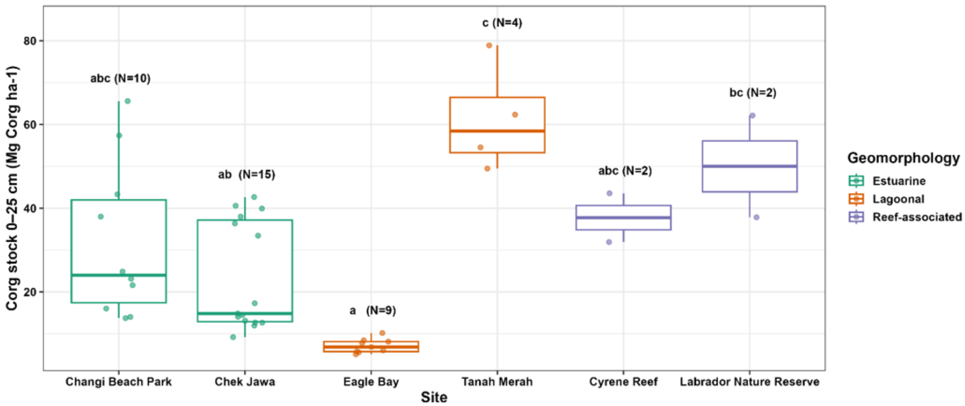

Formatted: Keep with next

Figure 2. Measured only 0–25 cm soil organic carbon stocks (Mg Corg ha−1) across sites, restricted to 0-25 cores (cores reaching ≥25 cm depth). Boxplots show medians and interquartile ranges; points show individual cores, coloured by geomorphology. Letters above sites indicate Tukey-adjusted differences in site estimated marginal means (emmeans; α = 0.05); sites sharing a letter are not significantly different. N indicates the number of 0-25 cm cores per site.

Formatted: Keep with next

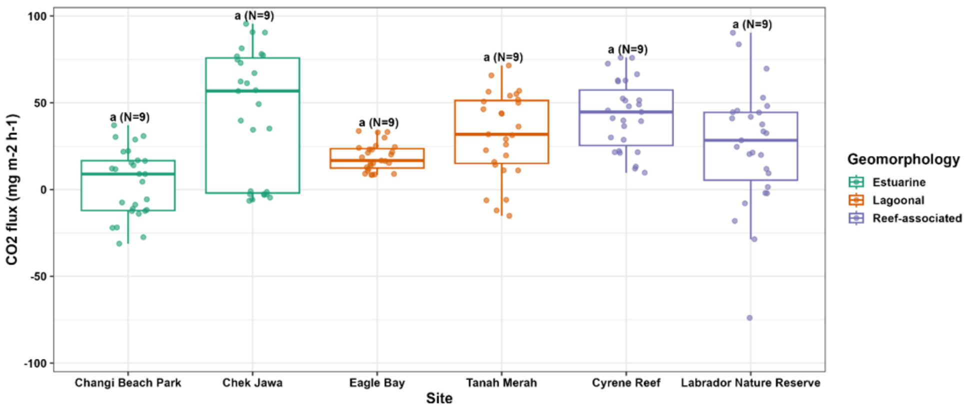

Figure 3. Sediment–air CO_2 flux (mg m−2 h−1) across sites during low-tide exposure (dark chambers). Boxplots show chamber-level flux distributions; points show individual chambers, coloured by geomorphology. The y-axis limits are symmetric (±max(|CO2|) across all chambers) to aid cross-site comparison. Letters above sites indicate Tukey-adjusted differences in site estimated marginal means from the site mixed model (emmeans; $\alpha = 0.05$); sites sharing a letter are not significantly different. N indicates the number of plots contributing flux measurements at each site.

Formatted: Keep with next

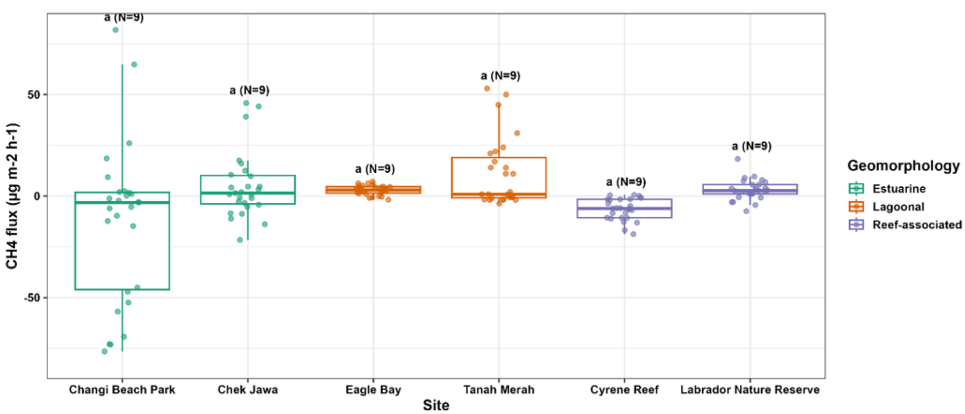

Figure 4. Sediment–air CH_4 flux (µg m−2 h−1) across sites during low-tide exposure (dark chambers). Boxplots show chamber-level flux distributions; points show individual chambers, coloured by geomorphology. The y-axis limits are symmetric (±max(|CH4|) across all chambers) to aid cross-site comparison. Letters above sites indicate Tukey-adjusted differences in site estimated marginal means from the site mixed model (emmeans; $\alpha = 0.05$); sites sharing a letter are not significantly different. N indicates the number of plots contributing flux measurements at each site.

Formatted: Caption

Formatted: English (Singapore)

3.2 Spatial variability in seagrass soil carbon stocks and fluxes

Intra-site heterogeneity in soil C_{org} % was observed, with significant plot-to-plot variation detected at 50% of the surveyed sites. Among sites, significant spatial differences in soil C_{org} % were recorded (KW test; n = 62, df = 5, $\chi 2$ = 45.67, p < 0.001). Tanah Merah had the highest C_{org}% at 2.5 ± 0.5% (Range: 1.8 to 3.6%), while Eagle Bay had the lowest concentrations at 0.2 ± 0.1% (Range: 0.1 to 0.4%, Figure 2a). Across geomorphic settings, soil C_{org} % differed significantly ($\chi 2$ = 28.9, p < 0.001), with values of 0.7 ± 0.4%, 1.3 ± 1.2% and 1.3 ± 0.4% recorded for estuarine, lagoonal and reef-associated seagrass systems, respectively (Figure 2b). Vertical distribution showed consistent decreases in C_{org} % across all geomorphic settings, with estuarine systems showing the smallest reduction (25% from 0.8% at the surface to 0.6% in the subsurface). Lagoonal systems had the strongest depth gradient, with surface C_{org}% of 1.5% declining by 40% to 0.9% in subsurface sediments, reaching particularly low values (0.2%) below 40 cm. Reef-associated systems showed intermediate patterns, with surface concentrations of 1.5% decreasing by 30% to 1% in deeper layers, indicating moderate C_{org} % preservation with depth.

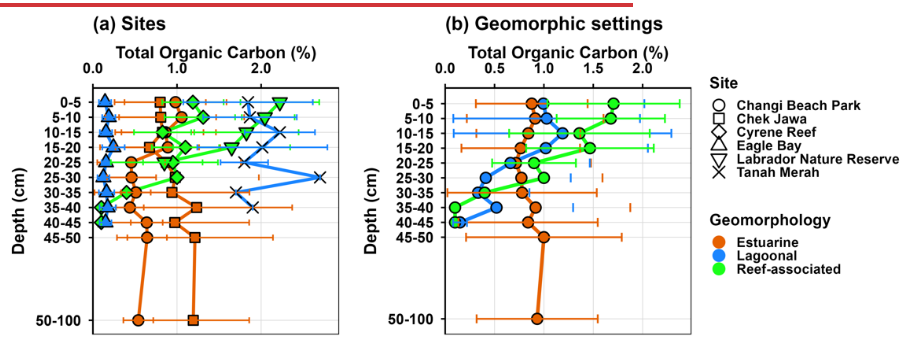

Figure 2: Seagrass soil total organic carbon % (mean ± SE) across spatial scales, including (a) sites and (b) geomorphic settings.

Overall, the carbon stocks recorded in the top 100 cm of seagrass meadows were 131.6 ± 77.6 Mg ha^{-1}, with Reef-associated meadows having the highest C_{org} stock of 180.8 ± 110.6 Mg ha^{-1}, followed by lagoonal sites at 131.9 ± 49.3 Mg ha^{-1} and estuarine meadows at 31.1 ± 17.3 Mg ha^{-1} (Figure 3a, b).

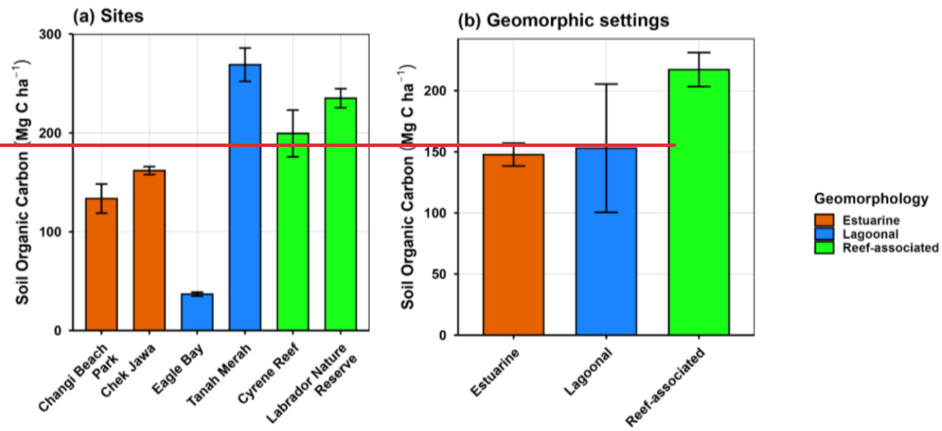

Figure 3: Seagrass soil organic carbon stocks (Mg ha-1, mean ± SE) across spatial scales, including (a) sites and (b) geomorphic settings.

At the intra-site level, soil CO_2 fluxes did not show significant intra-site variability in 67% of the surveyed sites. Soil CO_2 fluxes varied significantly among sites (KW test; n = 162, df = 5, $\chi 2$ = 35.7, $p < 0.001$, Figure 4a). The highest CO_2 fluxes were recorded at Chek Jawa at 42.5 ± 40.8 mg m^{-2} h^{-1} (Range: -24.8 to 104.8 mg m^{-2} h^{-1}) and the lowest at Changi Beach at 15.0 ± 15.3 mg m^{-2} h^{-1} (Range: -31.1 to 37.1 mg m^{-2} h^{-1}, Figure 4a). Among geomorphic settings, mean soil CO_2 fluxes did not vary significantly ($\chi 2$ = 2.33, p = 0.313) at 28.8 ± 33.6 mg m^{-2} h^{-1}, 30.0 ± 16.4 mg m^{-2} h^{-1} and 32.8 ± 30.6 mg m^{-2} h^{-1} for estuarine, lagoonal and reef-associated seagrasses, respectively (Figure 4b).

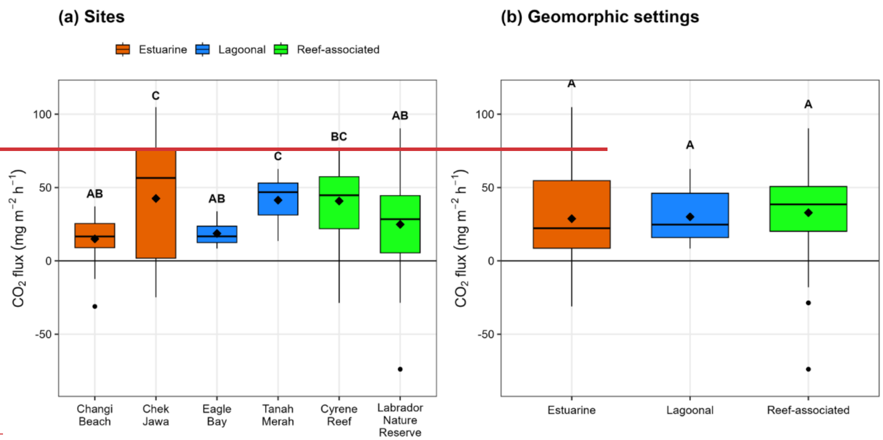

Figure 4: Seagrass soil carbon dioxide fluxes (mean ± SE) across spatial scales, including (a) sites and (b) geomorphic settings. Positive fluxes indicate emission into the air, while negative fluxes indicate uptake by the sediment. Different upper-case letters indicate significant differences ($p \leq 0.05$) across the sites and geomorphic settings following Dunn's test with Bonferroni correction.

At the intra-site level, soil CH_4 fluxes did not vary significantly for 83% of the measured sites. Soil CH_4 emissions varied significantly among sites (KW test; df = 5, $\chi 2 = 15.62$, $p = 0.008$, Fig. 5a). The highest CH_4 fluxes were recorded at Tanah Merah at 8.0 ± 21.2 µg m^{-2} h^{-1} (Range: -29.2 to 32.7 µg m^{-2} h^{-1}). Changi Beach and Cyrene Reef had the lowest CH_4 fluxes with an uptake of -6.7 ± 38.3 µg m^{-2} h^{-1} (Range: -76.5 to 81.8 µg m^{-2} h^{-1}, Fig. 5a) and -4.5 ± 8.7 µg m^{-2} h^{-1} (Range: -18.7 to 15.4 µg m^{-2} h^{-1}, Fig. 5a), respectively. Soil CH_4 emissions did not vary significantly among geomorphic settings (KW test; df = 2, $\chi 2 = 3.69$, $p = 0.158$; Fig. 5b). Mean CH_4 fluxes were -1.0 ± 30.2 µg m^{-2} h^{-1}, 4.7 ± 15.6 µg m^{-2} h^{-1} and -1.1 ± 9.5 µg m^{-2} h^{-1} for estuarine, lagoonal and reef-associated seagrasses, respectively.

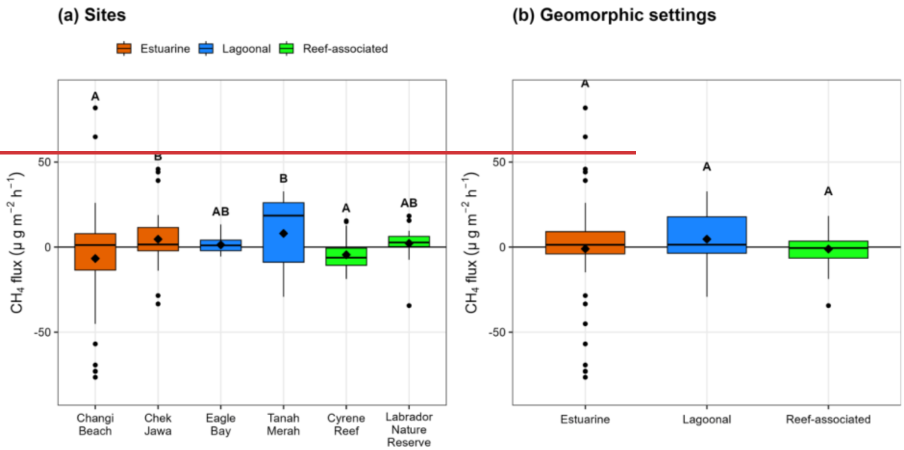

~~**Figure 5: Seagrass soil methane fluxes (mean ± SE) across spatial scales, including (a) sites and (b) geomorphic settings. Positive fluxes indicate emission into the air, while negative fluxes indicate uptake by the sediment. Different uppercase letters indicate significant differences (p ≤ 0.05) across sites and geomorphic settings, as determined by Dunn's test with a Bonferroni correction.**~~

Mixed-effects models accounting for the nested sampling design showed no evidence of differences among geomorphic settings in 0–25 cm stocks (Fig. 2; Type III Satterthwaite test: F (2,3.07) = 0.246, p = 0.796). CO_2 and CH_4 fluxes also did not differ among geomorphic settings in geomorphology-only models (CO_2, F (2,3.00) = 0.180, p = 0.844; CH_4, F *(2,3.00) = 0.844*, p = 0.513).

Sensitivity analyses for 0–100 cm stocks indicated a marginal geomorphology effect for measured-only totals (F *(2,2.65) = 8.114*, p = 0.074), but no effect after extrapolating all cores to 100 cm (F *(2,2.96) = 0.22*, p = 0.816). Refusal depth differed strongly among geomorphic settings (Supplement Table S2). Estuarine cores reached much greater depths (mean 97 ± 15.3 cm, n= 26) than lagoonal cores (mean 31.6 ± 10.7 cm; n= 18) and reef-associated cores (mean 18.7 ± 8.2 cm; n=18). In a mixed-effects model with site as a random intercept, refusal depth differed significantly among geomorphic settings, with lagoonal (estimate -65 cm p = 0.003) and reef-associated (estimate = -77.9 cm; p = 0.002) cores being shallower than estuarine cores (Supplement Table S2). Overall, 25 of 62 cores (40.3%) reached 100 cm depth, and 25 of 62 cores (40.3%) reached ≥80 cm depth (Supplement Table S2).

Variance partitioning indicated strong scale dependence in variability (Supplement Table S2): 0–25 cm stocks were dominated by site-level variance (72.30%), with additional variance among transects within sites (7.61%) and residual variance (20.09%). CO_2 variance was distributed across plot (16.96%), transect (29.03%), site (22.50%) and residual (31.50%) components, whereas CH_4 variance was concentrated at the plot scale (60.76%) with smaller site (10.99%) and residual (28.25%) components.

3.3 Relationship between carbon stocks and fluxes and environmental parameters

Seagrass soil cores from all sites contained, on average (± SD), 585.8 ± 293.8 µm grain size, 1.4 ± 0.3 g cm^{-3} dry bulk density, 0.9 ± 0.8 C_{org}% and 0.01 ± 0.01 g cm^{-3} soil C_{org} density in the top 100 cm. Grain size varied significantly across depth intervals (KW; df = 423, χ^2 = 41.4, p < 0.0001), (KW; df = 5, χ^2 = 184.7, p < 0.0001), sites (KW; df = 5, χ^2 = 184.7, p < 0.0001) and geomorphic settings (KW; df = 2, χ2 = 161.8, p < 0.0001). Grain size was larger >200 µm in the upper 30cm soil profile and decreased to <125 µm in the lower 40-100 cm soil profile (Fig. 6a). Across sites, Eagle Bay had a high grain size of 604.3 ± 254.7 µm, while Changi Beach Park had the lowest grain size of 99.1 ± 117.1 µm (Fig. 6a). Across geomorphic settings, estuarine sites had a significantly lower grain size of ~119.1 ± 137.7 µm followed by reef- associated at and lagoonal sites, which contained a grain size of 393.7 ± 283.9 µm and 517.1 ± 137.7 µm respectively (Fig. 6b).

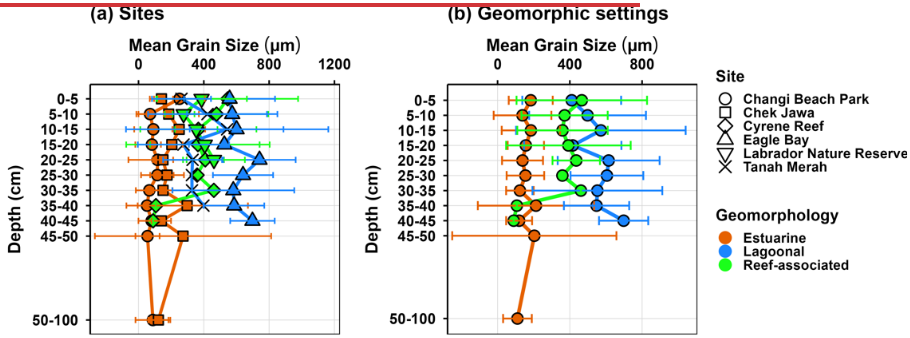

Figure 6: Seagrass soil grain size (mean ± SE) across spatial scales, including (a) sites and (b) geomorphic settings.

Dry bulk density did not show significant intra-site variability in 83% of the surveyed sites. However, significant spatial differences in soil DBD were observed among study sites (KW test; n = 62, df = 5, χ2 = 38.9, p < 0.001, Fig. 7a). Eagle Bay exhibited the highest DBD at 1.7 ± 0.1 g cm^{-3} (Range: 1.5 to 1.9 g cm^{-3}), while Tanah Merah had the lowest values at 0.9 ± 0.2 g cm^{-3} (Range: 0.7 to 1.3 g cm^{-3}, Fig. 7a). Across geomorphic settings, soil DBD differed significantly (df = 2, χ2 = 24.2, p < 0.001), with values of 1.5 ± 0.3 g cm^{-3}, 1.3 ± 0.4 g cm^{-3} and 1.4 ± 0.2 g cm^{-3} recorded for estuarine, lagoonal and reef-associated seagrass systems, respectively (Fig. 7b). Across depth profiles within geomorphic settings, estuarine and reef-associated seagrass meadows showed negligible to minimal change, while lagoonal meadows showed more variable depth profiles, with surface DBD of 1.3 g cm^{-3} increasing by 12% to 1.4 g cm^{-3} below 15 cm, though this pattern varied considerably between the two measured sites (Fig 6b).

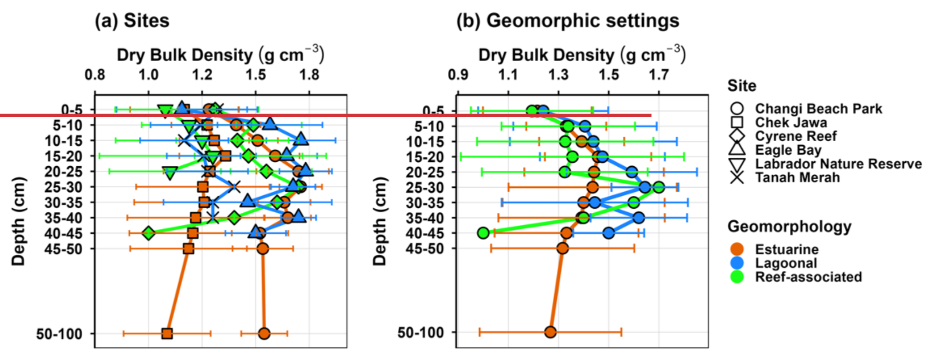

Figure 7: Seagrass soil dry bulk density (mean ± SE) across spatial scales, including (a) sites and (b) geomorphic settings.

Soil organic carbon density across seagrass ecosystems averaged 0.013 ± 0.008 g cm^{-3} (Range: 0.002 to 0.030 g cm^{-3}) for all study locations. Intra-site heterogeneity in soil SOC density was not significant for 67% of the surveyed sites. Significant spatial differences in soil SOC density were recorded among study sites (KW test; n = 62, df = 5, $\chi 2$ = 42.3, $p < 0.001$). Tanah Merah exhibited the greatest SOC density at 0.024 ± 0.003 g cm^{-3} (Range: 0.019 to 0.030 g cm^{-3}), while Eagle Bay displayed the lowest SOC density at 0.003 ± 0.001 g cm^{-3} (Range: 0.002 to 0.004 g cm^{-3}, Fig. 8a). Across geomorphic environments, soil SOC density differed significantly ($\chi 2$ = 26.7, $p < 0.001$), with values of 0.010 ± 0.005 g cm^{-3}, 0.013 ± 0.011 g cm^{-3} and 0.018 ± 0.005 g cm^{-3} recorded for estuarine, lagoonal and reef-associated seagrass systems, respectively (Fig. 8b). Vertical distribution patterns varied markedly among geomorphic settings, with estuarine systems maintaining uniform SOC throughout the profile at 0.011 g cm^{-3} for 0-15 cm top and 0.010 g cm^{-3} for >15 cm, representing only an 11% decrease. In contrast, lagoonal systems showed pronounced stratification with 37% SOC reduction from surface (0.013 g cm^{-3}) to subsurface (0.008 g cm^{-3}), reaching minimum values of 0.002 g cm^{-3} at 40-45 cm depth. Reef-associated systems exhibited the highest surface SOC at 0.019-0.022 g cm^{-3} in the top 0-10 cm but showed a 29% reduction in subsurface layers, with minimal SOC density at 0.001 g cm^{-3} below 35 cm depth.

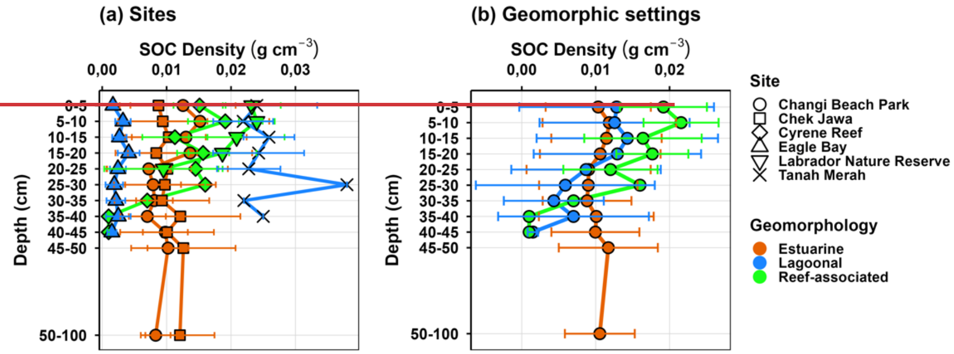

Figure 8: Seagrass soil organic carbon density (mean ± SE) across spatial scales, including (a) sites and (b) geomorphic settings.

We found carbon stocks were significantly and positively associated with soil temperature (ρ=0.59, q≈1.6e−05) and salinity (ρ=0.85, q≈2.9e−14, Fig. S1, S2). Soil temperature and salinity significantly co-varied (ρ=0.841, q≈3.9e−14), reflecting a shared gradient. Corg% decreased with bulk density (ρ=−0.35, q≈0.029) and increased with salinity (ρ=0.60, q≈1.0e−05). Redox was inversely associated with bulk density (ρ=−0.48, q≈1.0e−03). CO_2 flux was moderately negatively associated with C stocks (ρ=−0.33, q=0.0398) and significantly negatively correlated with median grain size (ρ=−0.68, q≈1.0e−07). Other CO_2 associations were marginal after FDR. CH_4 flux was moderately positively associated with carbon stocks (ρ=0.42, q=0.00499) but strongly correlated with C_{org}% (ρ=0.75, q≈1.1e−09). CH_4 flux decreased with bulk density (ρ=−0.58, q≈2.6e−05) and increased significantly with median grain size (ρ=0.54, q≈1.2e−04) and redox (ρ=0.74, q≈2.2e−09).

Multivariate model explained ~60% of variance in CO_2 fluxes (marginal R^2 = 0.60), with total variance explained ~79% (conditional R2 = 0.79; cross-validated mean R^2=−0.31). CO_2 flux increased with redox (β = +4.02 ± 1.18, p = 0.001) and decreased with dry bulk density (β = −4.44 ± 1.06, p < 0.001). Reef-associated (Δ = −16.85 ± 3.86, p < 0.001) and lagoonal (Δ = −6.95 ± 1.86, p < 0.001) meadows had lower CO_2 fluxes than estuarine. Despite strong bivariate correlations, C_{org}% and grain size were not significantly associated with CO_2 flux in the multivariate model, indicating confounding with structure/chemistry gradients. About ~80% of the variance (marginal R^2 = 0.80) in CH_4 flux was explained by the multivariate model, and cross-validation highlighted modest predictive skill across sites (mean R2 = 0.25). As expected, CH_4 flux increased with C_{org}% (standardised β = 0.36 ± 0.15, p = 0.021), with a higher increase rate in reef-associated (Δ = +1.63 ± 0.45, p < 0.001) and lagoonal (Δ = +0.66 ± 0.23, p = 0.007) meadows relative to estuarine. After accounting for the hierarchy and geomorphic settings, redox was a borderline predictor (p = 0.054), while dry bulk density, salinity, grain size, and soil temperature were not significant predictors of CH_4 flux.

Among tested sediment properties for 0-25 cm, mud % ranged from 2.5 to 97.9% and dry bulk density was 0.8 to 1.7 g cm-3 (see site and geomorphology level details in Table S3 and Fig S1). Across all sites, redox ranged from -91.6 to 156.7 mV, pH from 6.9 to 7.8, salinity from 22.4 to 31.3 psu, surface water temperature from 27.4 to 30.1 °C, conductivity from 33.4 to 48 mS/cm and dissolved oxygen from 34.9 to 97.7% (see site and geomorphology level details in Table S4 and Fig S2).

To explore drivers of site-dominated variability in 0–25 cm stocks, we fit an expanded core-level mixed model including depth-resolved sediment properties (0–25 cm mud fraction and dry bulk density) and plot-level environmental covariates (salinity, redox, pH, water temperature, dissolved oxygen). Predictors were centred within site (within-site effects) and transects were modelled as random intercepts nested within sites. None of the tested predictors were significant at $\alpha = 0.05$ (all $p \geq 0.073$); dissolved oxygen $p = 0.073$, and salinity ($p = 0.099$ were marginal (Supplement Table S2; StockDrv_Expanded sheets).

In the multivariate CO_2 driver model, geomorphology showed an overall effect (Type III Satterthwaite test: F (2,16.42) = 4.54, $p = 0.027$). Water temperature was a significant negative predictor (Type III Satterthwaite test: F 1,16.47) = 8.12, $p = 0.011$ while dissolved oxygen was marginal ($p = 0.081$). Redox, salinity, pH, and mud fraction were not significant (all $p > 0.158$). Tukey-adjusted pairwise contrasts are reported in Supplement Table S2. A sensitivity model removing the site random intercept produced an identical likelihood (likelihood-ratio test $p = 1.0$ and slightly improved AIC (1467.866 vs 1469.866), indicating robust fixed-effect inference (Supplement Table S2).

In the multivariate CH_4 driver model, no predictors were significant, including C_{org} ($p = 0.298$), redox ($p = 0.703$), salinity ($p = 0.262$) and mud % ($p = 0.158$). At the plot level (plot-summed 0–25 cm stock vs plot-mean flux) with site as a random intercept, CO_2 flux decreased significantly with increasing plot-level stocks (β = -8.61, 95% CI = [-17.0, -0.26], $p = 0.044$: Fig. 5a). CH_4 flux showed no detectable association with 0–25 cm stock in the analogous plot-level model (β = -2.25, 95% CI = [8.57, 4.06], $p = 0.469$: Fig. 5b). Geomorphology contrasts were not significant for both CO_2 and CH_4 (all $p \geq 0.399$).

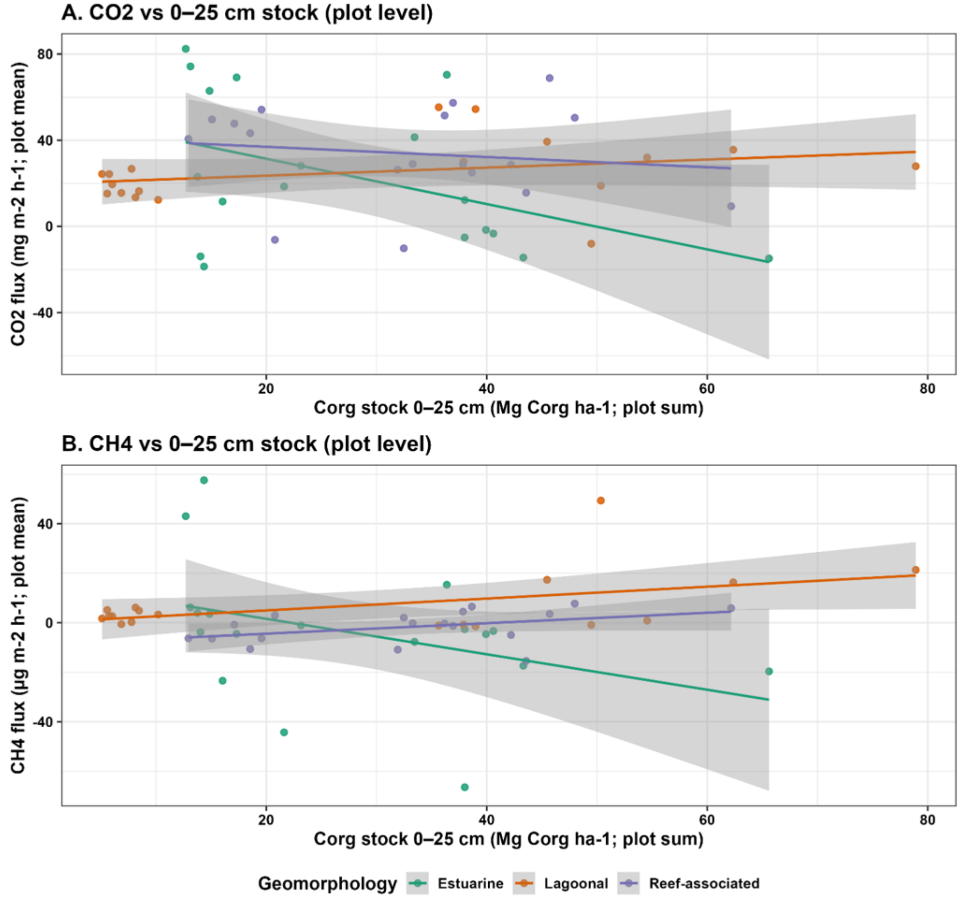

Figure 5. Plot-level relationships between measured 0–25 cm Corg stocks (plot-summed) and plot-mean greenhouse gas fluxes. Panel (A) shows CO2 versus 0–25 cm Corg stock; panel (B) shows CH4 versus 0–25 cm Corg stock. Points represent plots coloured by geomorphology; lines show linear fits with 95% confidence bands. Statistical inference is based on mixed-effects models that included geomorphology as a fixed effect and a random intercept for site.

Formatted: Keep with next

Formatted: Line spacing: single

4 Discussion

This study shows that tropical intertidal seagrass meadows in Singapore function as an important but highly spatially variable component of the coastal carbon cycle. This study quantifies near-surface (0–25 cm) soil organic carbon stocks and low-tide sediment–air CO_2 and CH_4 fluxes across six intertidal seagrass meadows in Singapore. Using a measured only 25 cm definition for near-surface stocks, geomorphology did not explain variation in 0–25 cm C_{org} stocks in mixed-effects models. Similarly, geomorphology-only models detected no setting differences in greenhouse gas fluxes (CO_2 and CH_4). However, in the multivariate CO_2 driver model that accounted for covarying environmental conditions (including temperature, oxygen and sediment texture), geomorphology showed an overall effect. This suggests that geomorphic settings may influence CO_2 flux indirectly through linked environmental gradients even when differences are not detectable in simpler setting-only tests. Our results highlight the necessity of spatially explicit carbon accounting that distinguishes between the drivers of storage and emissions to value these ecosystems in climate mitigation frameworks.

4.1 Soil carbon stocks and fluxes of tropical seagrass meadows in Singapore

Our soil organic carbon stocks for the top 15 and 30 cm fall within the ranges reported for local and global ~~regional~~ seagrass meadows (Table 1). Although our measured 100 cm soil organic carbon stocks are almost half of those reported for global seagrass meadows, they are consistent with those reported for the Halophila genus globally (Krause et al., 2025b). These findings situate intertidal seagrass meadows of Singapore as low to moderate carbon stores. The fluxes of CO_2 measured in this study are within the range of 5 to 920 mg m^{-2} h^{-1}, reported for seagrasses in South and Southeast Asia (Stankovic et al., 2023; Zheng et al., 2023). An important observation from this study was the presence of negative fluxes from dark chambers, which had not been reported previously for seagrasses. However, this has been observed in other coastal ecosystems and linked to the presence of novel microbiota that can respire in the absence of light. This microbiota included acetogens, chemosynthetic microbes able to sequester CO_2 in dark conditions ((Rodriguez et al., 2025). The potential presence of similar chemosynthetic microbes in the seagrass ecosystem suggests a yet unconstrained mechanism of CO_2 sequestration. CH_4 emissions were within the lower range of reported values of sediment-water and sediment-air CH_4 fluxes for tropical and temperate seagrasses in the region and globally (Asplund et al., 2022; Henriksson et al., 2024; Zheng et al., 2023). The relatively low CH_4 emissions in our study may be due to the presence of CH_4 consumption processes in the sediments of tropical seagrass meadows. Marine sediments are inhabited by sulphfate-reducing bacteria and methane-oxidising archaea that are known to efficiently oxidise CH_4 produced in sediments before it is released into the atmosphere (Orphan et al., 2001). These bacterial communities may consume up to 90% of the CH_4 produced in marine sediments (Reeburgh, 2007). Our findings show that tropical seagrasses are sinks or negligible sources of CH_4.

Table 1. Comparison of seagrass soil carbon stocks with previous estimates.

Formatted: Normal, Line spacing: single

Formatted: Superscript

Formatted: Superscript

References	Number of cores	Scale	Location	Mean ± SD Mg C_{org} ha^{-1} (median)	Min-Max Mg C_{org} ha^{-1}
Top 15 cm comparison					
This study, Estuarine	26	Landscape	Singapore	16.8 ± 10.1 (13.7)	6.1 to 43.4
This study, Lagoonal	18	Landscape	Singapore	19.9 ± 17 (17.5)	2.2 to 48.4
This study, Reef-associated	15	Landscape	Singapore	29.2 ± 8 (28.3)	15.1 to 43.7
Alemu et al. (2022), Estuarine	9	Landscape	Singapore	14.6 ± 12.6 (11.3)	4 to 28.6
Alemu et al. (2022), Lagoonal	9	Landscape	Singapore	25.2 ± 18.7 (19.6)	9.9 to 46.1
Alemu et al. (2022), Reef-associated	9	Landscape	Singapore	30.9 ± 37.3 (17.9)	4.1 to 83.6
Top 30 cm comparison					
This study measured only	35	Landscape	Singapore	28.4 ± 21.7 (18.9)	6.2 to 97.8
Mazarrasa et al. (2021)	43	Bioregion (Tropical)		20.3 ± 1.5	-
Kennedy et al. (2022)	576	Global	Global	33.5 ± 1.2	-
Krause et al. (2025b)	1022	Global	Global	41.1 ± 1.8	-
Top 100 cm comparison					
This study including predicted	62	Landscape	Singapore	124 ± 77.5 (121)	11.6 to 275.6
This study measured only	25	Landscape	Singapore	101 ± 43.5 (84.7)	29.1 to 169.5
Phang et al. (2015)	20	Local (site)	Singapore	138 ± 8.6	-
Stankovic et al. (2021)	-	Regional	Southeast Asia		0.10 to 205
Krause et al. (2025b)	227	Global	Global	194.3± 13.4 (145)	-

4.2 Scale-dependent variability in seagrass soil carbon stocks and fluxes

Across the primary geomorphology-only models, geomorphic setting was not a significant predictor of 0–25 cm stocks or of CO_2 and CH_4 fluxes. In contrast, geomorphology showed an overall effect in the multivariate CO_2 driver model after accounting for covariates, indicating that geomorphology may emerge through covarying environmental conditions rather than as a standalone setting effect. This indicates that, for the measured 0–25 cm stock response and the chamber fluxes analysed here, broad geomorphic classifications explain little additional variance beyond the site and within-site structure captured by

Formatted: Font: 10 pt, Not Bold

Formatted: Line spacing: 1.5 lines

the random effects. This is contrary to previous findings where geomorphic settings appeared as a strong predictor of 0-15 cm soil C_{org} stocks (Alemu et al., 2022), suggesting that geomorphic gradients may not be distinct enough due to the limited number of sites for each category or the influence of geomorphology may be overwhelmed by other factors. Refusal depth provides an informative indicator of sediment deposit thickness and potential capacity for deeper carbon storage. The strong geomorphology signal in refusal depth supports recommendations to report a common measured depth for primary inference in seagrass sediments and to treat deeper extrapolated estimates as sensitivity analyses. In our dataset, refusal depth patterns suggest that apparent differences in deeper (0–100 cm) stocks can partly reflect deposit thickness and sampling refusal rather than differences in near-surface carbon density alone.

Our findings highlight strong spatial variability in soil C_{org} stocks at the site level, which is consistent with differences in site history, disturbance, and terrestrial (allochthonous) inputs. Egale Bay, a reclaimed site with intensive recreational use, exhibited the lowest C_{org} stocks, whereas Tanah Merah—an engineered sandy lagoon behind coastal revetments that receives substantial terrestrial inputs via a major drain—showed the highest C_{org} stocks.

Our findings highlight strong spatial variability in soil C_{org} stocks, with geomorphic setting emerging as a primary control at the landscape scale. Reef-associated and lagoonal meadows stored substantially more carbon than estuarine sites in the upper 30 cm soil profile (Table 1), consistent with the limited hydrodynamic energy environments of reef-associated and lagoonal meadows creating depositional conditions which favour carbon storage and retention (Kennedy et al., 2022; York et al., 2018). In contrast, estuarine meadows showed lower storage, similar to patterns reported in other estuarine meadows (Carruthers et al., 2007; Alemu et al., 2022). Despite large amounts of terrestrial runoff, site-specific exposure to strong hydrodynamic energy and sediment dynamics, such as resuspension of fine sediment, may reduce net C_{org} stocks in estuarine sites (Mazarrasa et al., 2023). At the site scale, differences in salinity and bulk density contributed to variability in carbon stocks. Sites with higher salinity and lower bulk density had higher C_{org}, aligning with global evidence that salinity and sediment characteristics influence carbon retention (Miyajima et al., 2015; Kauffman et al., 2020; Serrano et al., 2019). High intra-site variability was likely due to patchiness in seagrass cover, species composition, and microtopography and species diversity. Seagrass species composition, cover, and canopy structure can influence sediment trapping, organic matter retention, and oxygen transport to sediments, thereby affecting both C_{org} storage (Kennedy et al., 2022; Krause et al., 2025a). and GHG production/oxidation. Although species traits were not explicitly modelled here, differences in meadow structure within and across sites could contribute to within-site and setting heterogeneity (Krause et al., 2025b) and should be incorporated in future trait-based blue carbon assessments. In our study, for instance, although *Halophila* spp. was dominant at both estuarine locations, Chek Jawa had higher diversity and C_{org} stocks than Changi Beach Park. Consistent with their C_{org} storage patterns, lagoonal and reef-associated meadows supported larger, high-biomass species (*Thalassia* spp. and *Cymodocea* spp.), contrasting with the smaller, low-biomass flora of estuarine sites (Table S4). This heterogeneity underscores the importance of adequate replication in sampling design to avoid misrepresentation of local stocks (Dahl et al., 2025). Generally, reef-associated and lagoonal meadows stored substantially more carbon than estuarine sites in the upper 15 cm soil profile (Table 1), consistent with the

Formatted: Line spacing: 1.5 lines

limited hydrodynamic energy environments of reef-associated and lagoonal meadows creating depositional conditions which favour carbon storage and retention (Kennedy et al., 2022; York et al., 2018). In contrast, estuarine meadows showed lower storage, similar to patterns reported in other estuarine meadows (Carruthers et al., 2007; Alemu et al., 2022). Despite large amounts of terrestrial runoff, site-specific exposure to strong hydrodynamic energy and sediment dynamics, such as resuspension of fine sediment, may reduce net C_{org} stocks in estuarine sites (Mazarrasa et al., 2023). In estuarine habitats, a balance of oceanic exchange and freshwater inflows creates a gradient in temperature, salinity and light that drives high variability in seagrass communities, which can influence intra-site C_{org} stocks in estuarine habitats (Carruthers et al., 2007; Alemu et al., 2022).

GHG fluxes exhibited substantial fine-scale heterogeneity. CO_2 variability was distributed across plot, transect, site, and residual components, while CH_4 variability was concentrated primarily at the plot scale, consistent with strong micro-scale patchiness and/or measurement-scale variability within sites. Similar to Unlike soil C_{org} storage, CO_2 and CH_4 fluxes showed limited variation across geomorphic settings at the landscape scale of Singapore, which exhibits a small represents an intermediate level due to its seagrass spatial extent of 229.6 ha (Tan et al., 2022) thus represents an intermediate landscape scale. GHG fluxes were relatively consistent, suggesting that at intermediate landscape scales, either GHG dynamics may be regulated by biogeochemical processes that are not influenced by geomorphology, geomorphic gradients may not be distinct enough at this scale, or the influence of geomorphology may be overwhelmed by other .factors. Emissions were relatively consistent, suggesting that at intermediate landscape scales, either GHG dynamics may be regulated by biogeochemical processes that are not influenced by geomorphology, geomorphic gradients may not be distinct enough at this scale, or the influence of geomorphology may be overwhelmed by other factors. Kirwan et al. (2023) proposed that fluxes are largely controlled by small-scale and short-term ecological and biogeochemical dynamics. Ecological processes such as species composition, plant productivity, electron acceptor availability and oxygen transport between soil and atmosphere can govern GHG fluxes in blue carbon ecosystems (Rosentreter et al., 2021). Our findings highlight that surface 25 cm carbon stock variability cannot be explained by geomorphic setting alone, in an intermediate landscape context and fluxes can appear similar across sites because they track production and deposition rather than long-term preservation dynamics.

geomorphic processes constrain carbon stocks, whereas fluxes are largely controlled by small-scale and short-term ecological and biogeochemical dynamics. Geomorphic settings, including estuaries, deltas, lagoons, etc., establish unique sedimentary processes that influence environmental parameters such as sediment supply, organic matter decomposition and persistent anoxia; all of which ultimately control long-term carbon storage in blue carbon ecosystems (Twilley et al., 2018). By contrast, ecological processes such as species composition, plant productivity, electron acceptor availability and oxygen transport between soil and atmosphere can govern GHG fluxes in blue carbon ecosystems (Rosentreter et al., 2021). Our findings highlight that carbon stock variability can be explained by geomorphic settings (estuarine vs barrier-lagoon systems, sediment

Formatted: Font: 10 pt, Not Bold

Formatted: Font: 10 pt, Not Bold

Formatted: Font: 10 pt, Not Bold

Formatted: Line spacing: 1.5 lines

Formatted: Font: 10 pt, Not Bold

Formatted: Font: 10 pt, Not Bold

Formatted: Font: 10 pt, Not Bold

supply, tidal range) even in an intermediate landscape context, while fluxes can appear similar across sites because they track production and deposition rather than long-term preservation dynamics.

4.3 Patterns and environmental controls on soil carbon stocks and fluxes

Our expanded core-level mixed model found that none of the tested sediment properties (mud fraction, bulk density) or plot-level environmental covariates explained site-dominated variability in 0-25 cm carbon stock. Although mud fraction is suggested as a proxy for intertidal seagrass meadows carbon stocks (Serrano et al., 2016), mud% was not a significant predictor of near-surface stocks or fluxes in our models, suggesting site-scale controls and unmeasured factors, e.g., hydrodynamic regime, deposit thickness, and species-specific traits (Kennedy et al., 2022) may be more important than within-site texture gradients in this system, rather than the within-site gradients captured by the measured physicochemical variables. In the multivariate CO_2 driver model, water temperature was the only significant predictor (negative effect), while mud %, redox, salinity, and pH were not significant and dissolved oxygen was marginal. The negative temperature relationship likely reflects temperature acting as a proxy for co-varying conditions (e.g., exposure/inundation state, timing within the low-tide window, or other unmeasured gradients) rather than a simple direct respiration-temperature response. For CH_4, none of the standardised predictors (including C_{org}%, mud %, redox, and salinity) was significant in the final driver model. These findings are consistent with previous studies where none of the potential drivers of vegetated coastal ecosystems, such as salinity, organic matter or biomass etc were associated with seagrass fluxes (Al-Haj and Fulweiler, 2020). Nonetheless, together with the variance partitioning (dominant plot-scale variance), this supports the interpretation that CH_4 fluxes in these intertidal meadows are highly heterogeneous at fine spatial scales and may require additional predictors e.g., microtopography, sulfate availability, plant traits, or episodic hydrologic forcing) and/or high-resolution temporal replication to resolve robust drivers. Overall, these findings reflect the nuanced interplay between environmental parameters and biogeochemical processes at multiple spatial scales, highlighting the importance of habitat-specific factors in controlling GHG emissions and organic carbon dynamics in tropical seagrass meadows and their implications for blue carbon budgets.

The bivariate patterns suggest that sites along a shared salinity–temperature gradient accumulate more carbon, with carbon stocks rising alongside both salinity and soil temperature, and salinity–temperature themselves strongly co-vary. This is consistent with the previous findings reporting higher soil C_{org}% in marine seagrass meadows (comparatively saltier) than estuarine meadows (Juma et al., 2020) and increasing salinisation increased soil carbon storage in seagrass meadows (Ruiz-Fernández et al., 2020). Mechanistically, saltier, warmer, and typically more marine-influenced meadows may favour higher organic matter retention and slower mineralisation, especially where lower bulk density indicates looser, potentially finer, and more organic-rich sediments. These background gradients help explain the flux patterns in our study: CO_2 flux is higher when redox is higher (more oxidising) and lower when bulk density is higher, indicating aerobic respiration is a dominant pathway for CO_2 production where oxygen availability is greater, and sediments are less compact. Our data did not show a direct correlation between soil C_{org} stocks and CO_2 fluxes, suggesting that high carbon storage does not necessarily imply elevated

Formatted: Font: 10 pt, Not Bold
Formatted: Line spacing: 1.5 lines
Formatted: Font: 10 pt, Not Bold
Formatted: Font: 10 pt, Not Bold
Formatted: Font: 10 pt, Not Bold
Formatted: Font: 10 pt, Not Bold
Formatted: Font: 10 pt, Not Bold
Formatted: Font: 10 pt, Not Bold

CO_2 emissions. Methane emissions appear more tightly linked to the quantity and perhaps nature of organic substrate than to the broader physical gradients once hierarchical structure is considered. The multivariate model confirms C_{org}% as a significant predictor (standardised β≈0.36) of CH_4 flux. Though not significant, reef-associated and lagoonal meadows showed slightly higher CH_4 flux relative to estuarine, aligning with their relatively higher organic content and perhaps microbially favourable conditions for methanogenesis. This indicates CH_4 production as a function of organic matter quantity, which is regulated by localized redox conditions and microbial processes (Al-Haj and Fulweiler, 2020). Overall, these findings reflect the nuanced interplay between environmental parameters and biogeochemical processes at multiple spatial scales, highlighting the importance of habitat-specific factors in controlling GHG emissions and organic carbon dynamics in tropical seagrass meadows and their implications for blue carbon budgets.

5 Conclusions

This study advances understanding of tropical seagrass carbon dynamics by quantifying soil organic carbon stocks and greenhouse gas fluxes across multiple spatial scales in Singapore. We show that 0-25 cm soil C_{org} stocks are highly variable but do not differ among geomorphic setting in mixed-effects models. Geomorphology-only models similarly show no setting differences in CO_2 or CH_4 fluxes. In contrast, multivariate driver modelling indicates that CO_2 flux is associated with environmental gradients, with temperature as a significant predictor and an overall geomorphology effect after accounting for covariates, whereas CH_4 flux drivers were not resolved with the variables included. Refusal depth differed strongly among geomorphic settings, highlighting that sediment deposit thickness varies systematically across environments and supporting the use of common-depth primary inference alongside clearly labelled deeper sensitivity estimates. These findings underscore the importance of sampling designs and analyses that reflect nested spatial structure and of jointly considering carbon storage and greenhouse gas fluxes in robust coastal carbon accounting.

soil C_{org} storage is highly variable, with geomorphic setting acting as a dominant control at the landscape scale; intra-site heterogeneity in soil C_{org} highlights the importance of adequate sampling to capture spatial variability; and greenhouse gas emissions (CO_2 and CH_4) are relatively uniform across settings, and CH_4 fluxes directly correspond to carbon storage levels.

Our results underscore two important implications for blue carbon accounting. First, soil C_{org} storage in tropical seagrasses is highly variable and strongly influenced by geomorphic settings, highlighting the need for spatially explicit approaches to stock estimation. Applying global averages to local contexts risks substantial under- or overestimation, with consequences for policy and carbon market applications (Dahl et al., 2025). Second, since GHG fluxes complicate and can reduce the climate benefits of blue carbon ecosystems (Malerba et al., 2022), accounting for GHG fluxes, particularly CH_4 emissions, is important for understanding the climate change mitigation potential of seagrass ecosystems.

Our findings contribute critical baseline data from Southeast Asia—a region of high seagrass biodiversity but limited empirical data. They also provide a methodological framework for other small island states with comparable seascapes. Importantly, our study demonstrates that while tropical seagrasses can store substantial carbon, this ecosystem function is context-dependent, shaped by ~~geomorphology and~~ site-specific factors. Accounting for such variability is essential for robust integration of seagrasses into national and global climate strategies.

Data availability

Data access can be requested from the corresponding author.

Author contributions

Lian Pin Koh and Daniel A. Friess, funding acquisition; Naima Iram, Daniel A. Friess, Lian Pin Koh, and Kiah Eng Lim, conceptualising; Naima Iram, Kiah Eng Lim, Muhammad Ariq Khalingga, Sheryl Chan Si Ern and Pierre Taillardat, sampling and laboratory analysis, Naima Iram Muhammad, Ariq Khalingga data analysis, Naima Iram and Daniel A. Friess writing the first draft, and all authors contributed to the final draft.

Competing interests

The contact author has declared that neither of the authors has any competing interests.

Acknowledgements

We thank Daisuke Taira, Jamie Yeo, Dr Tan Zu Dienle, Pavarne Shantti Sivalingam, Hao Tang and other colleagues and volunteers from the Centre for Nature-based Climate Solutions (National University of Singapore) and the Mangrove Lab (Tulane University and National University of Singapore) for their support during the work. We thank Serena Teo and Ow Yan Xiang for comments during the development of the project.

Financial support

This research was supported by Temasek and by the Singapore National Research Foundation grant entitled ‘‘A Blue Carbon Framework for Singapore’s National Climate Change Policy” (NRF-MCCS21-1-1-0001).

NI, KEL, MAK and SCSE were supported by Temasek.

References

Al-Haj, A. N. and Fulweiler, R. W.: A synthesis of methane emissions from shallow vegetated coastal ecosystems, 10.1111/gcb.15046, 2020.

Alemu, J. B., Yaakub, S. M., Yando, E. S., San Lau, R. Y., Lim, C. C., Puah, J. Y., and Friess, D. A.: Geomorphic gradients in shallow seagrass carbon stocks, Estuarine, Coastal and Shelf Science, 265, 107681, 2022.

Asplund, M. E., Bonaglia, S., Boström, C., Dahl, M., Deyanova, D., Gagnon, K., Gullström, M., Holmer, M., and Björk, M.: Methane Emissions From Nordic Seagrass Meadow Sediments, Frontiers in Marine Science, 8, 10.3389/fmars.2021.811533, 2022.

Bates, D., Mächler, M., Bolker, B., and Walker, S.: Fitting Linear Mixed-Effects Models Using lme4, Journal of Statistical Software, 67, 1–48, 10.18637/jss.v067.i01, 2015.

Burkholz, C., Garcias-Bonet, N., and Duarte, C. M.: Warming enhances carbon dioxide and methane fluxes from Red Sea seagrass (Halophila stipulacea) sediments, Biogeosciences, 17, 1717–1730, 10.5194/bg-17-1717-2020, 2020.

Capece, L. R., Griffin, A. J., Ward, M. A., Ricart, A. M., Shukla, P., Lobrutto, J., and Hill, T. M.: Multi-Scale Variability of Blue Carbon in Seagrass Sediments From Three California Estuaries, Journal of Geophysical Research: Biogeosciences, 130, 10.1029/2024jg008526, 2025.

Carruthers, T. J. B., Dennison, W. C., Kendrick, G. A., Waycott, M., Walker, D. I., and Cambridge, M. L.: Seagrasses of south–west Australia: A conceptual synthesis of the world's most diverse and extensive seagrass meadows, Journal of Experimental Marine Biology and Ecology, 350, 21–45, 10.1016/j.jembe.2007.05.036, 2007.

Dahl, M., Lavery, P. S., Mazarrasa, I., Samper-Villarreal, J., Adame, M. F., Crooks, S., Duarte, C. M., Friess, D. A., Krause-Jensen, D., Leiva-Dueñas, C., Lovelock, C. E., Macreadie, P. I., Masqué, P., Mateo, M. A., and Serrano, O.: Recommendations for strengthening blue carbon science, One Earth, 8, 10.1016/j.oneear.2025.101175, 2025.

do Amaral Camara Lima, M., Bergamo, T. F., Ward, R. D., and Joyce, C. B.: A review of seagrass ecosystem services: providing nature-based solutions for a changing world, Hydrobiologia, 850, 2655–2670, 10.1007/s10750-023-05244-0, 2023.

Duarte, C. M., Apostolaki, E. T., Serrano, O., Steckbauer, A., and Unsworth, R. K. F.: Conserving seagrass ecosystems to meet global biodiversity and climate goals, Nature Reviews Biodiversity, 1, 150–165, 10.1038/s44358-025-00028-x, 2025.

Gomis, E., Strydom, S., Foster, N. R., Montemayor, D., Mateo, M. A., Serrano, E., Inostroza, K., McCallum, R., Lafratta, A., Webster, C. L., O'Dea, C. M., Said, N. E., Dunham, N., Bernasconi, R., Werner, A., Vitelli, F., Puigcorbe, V., D'Cruz, A., Salinas, C., McMahon, K. M., Hyndes, G. A., Lavery, P. S., Pessarodona, A., Duarte, C. M., and Serrano, O.: Global estimates of seagrass blue carbon stocks in biomass and net primary production, Nature Communications, 16, 9530, 10.1038/s41467-025-64667-6, 2025.

Guerra-Vargas, L. A., Gillis, L. G., and Mancera-Pineda, J. E.: Stronger together: do coral reefs enhance seagrass meadows “blue carbon” potential?, Frontiers in Marine Science, 7, 628, 2020.

Henriksson, L., Yau, Y. Y. Y., Majtényi-Hill, C., Ljungberg, W., Tomer, A. S., Zhao, S., Wang, F., Cabral, A., Asplund, M., and Santos, I. R.: Drivers of Seasonal and Diel Methane Emissions From a Seagrass Ecosystem, Journal of Geophysical Research: Biogeosciences, 129, 10.1029/2024jg008079, 2024.

Howard, J., Hoyt, S., Isensee, K., Telszewski, M., and Pidgeon, E.: Coastal blue Carbon: Methods for assessing carbon stocks and emissions factors in mangroves, tidal salt marshes, and seagrasses, Conservation International, Intergovernmental Oceanographic Commission of UNESCO, International Union for Conservation of Nature, Conservation International, Intergovernmental Oceanographic Commission of UNESCO, International Union for Conservation of Nature, Virginia, USA, 10.2307/2674772, 2014.

Howard, J., Hoyt, S., Isensee, K., Pidgeon, E., Telszewski, M. (eds.): Coastal Blue Carbon: Methods for assessing carbon stocks and emissions factors in mangroves, tidal salt marshes, and seagrass meadows, Conservation International, Intergovernmental Oceanographic Commission of UNESCO, International Union for Conservation of Nature. Arlington, Virginia, USA., 2014.

Iram, N., Maher, D. T., Lovelock, C. E., Baker, T., Cadier, C., and Adame, M. F.: Climate change mitigation and improvement of water quality from the restoration of a subtropical coastal wetland, Ecological Applications, 10.1002/eap.2620, 2022.

Juma, G. A., Magana, A. M., Michael, G. N., and Kairo, J. G.: Variation in Seagrass Carbon Stocks Between Tropical Estuarine and Marine Mangrove-Fringed Creeks, Frontiers in Marine Science, 7, 10.3389/fmars.2020.00696, 2020.

Kauffman, J. B., Adame, M. F., Arifanti, V. B., Schile-Beers, L. M., Bernardino, A. F., Bhomia, R. K., Donato, D. C., Feller, I. C., Ferreira, T. O., Jesus Garcia, M. d. C., MacKenzie, R. A., Megonigal, J. P., Murdiyarso, D., Simpson, L., and Hernández Trejo, H.: Total ecosystem carbon stocks of mangroves across broad global environmental and physical gradients, Ecological Monographs, 90, 10.1002/ecm.1405, 2020.

Kennedy, H., Pagès, J. F., Lagomasino, D., Arias-Ortiz, A., Colarusso, P., Fourqurean, J. W., Githaiga, M. N., Howard, J. L., Krause-Jensen, D., Kuwae, T., Lavery, P. S., Macreadie, P. I., Marbà, N., Masqué, P., Mazarrasa, I., Miyajima, T., Serrano, O., and Duarte, C. M.: Species Traits and Geomorphic Setting as Drivers of Global Soil Carbon Stocks in Seagrass Meadows, Global Biogeochemical Cycles, 36, 10.1029/2022gb007481, 2022.

Kirwan, M. L., Megonigal, J. P., Noyce, G. L., and Smith, A. J.: Geomorphic and ecological constraints on the coastal carbon sink, Nature Reviews Earth & Environment, 4, 393–406, 10.1038/s43017-023-00429-6, 2023.

Krause, J. R., Chroeng, C., Glue, M., Mesa, L., Ngoun, T., Tak, C., Bayley, D. T. I., and Fourqurean, J. W.: The influence of seagrass traits and environmental controls on soil organic carbon stocks in Chrouy Pros Bay, Cambodia, Sci Total Environ, 993, 180000, 10.1016/j.scitotenv.2025.180000, 2025a.

Krause, J. R., Cameron, C., Arias-Ortiz, A., Cifuentes-Jara, M., Crooks, S., Dahl, M., Friess, D. A., Kennedy, H., Lim, K. E., Lovelock, C. E., Marba, N., McGlathery, K. J., Oreska, M. P. J., Pidgeon, E., Serrano, O., Vanderklift, M. A., Wong, L. W., Yaakub, S. M., and Fourqurean, J. W.: Global seagrass carbon stock variability and emissions from seagrass loss, Nature Communications, 16, 3798, 10.1038/s41467-025-59204-4, 2025b.

Kuznetsova, A., Brockhoff, P. B., and Christensen, R. H. B.: lmerTest Package: Tests in Linear Mixed Effects Models, Journal of Statistical Software, 82, 1–26, 10.18637/jss.v082.i13, 2017.

Lavery, P. S., Mateo, M.-Á., Serrano, O., and Rozaimi, M.: Variability in the carbon storage of seagrass habitats and its implications for global estimates of blue carbon ecosystem service, PloS one, 8, e73748, 2013.

Lenth, R. V. and Piaskowski, J.: emmeans: Estimated Marginal Means, aka Least-Squares Means, 10.32614/CRAN.package.emmeans, 2026.

Macreadie, P. I., Costa, M. D. P., Atwood, T. B., Friess, D. A., Kelleway, J. J., Kennedy, H., Lovelock, C. E., Serrano, O., and Duarte, C. M.: Blue carbon as a natural climate solution, Nature Reviews Earth & Environment, 2, 826–839, 10.1038/s43017-021-00224-1, 2021.

Malerba, M. E., Friess, D. A., Peacock, M., Grinham, A., Taillardat, P., Rosentreter, J. A., Webb, J., Iram, N., Al-Haj, A. N., and Macreadie, P. I.: Methane and nitrous oxide emissions complicate the climate benefits of teal and blue carbon wetlands, One Earth, 5, 1336–1341, 10.1016/j.oneear.2022.11.003, 2022.

Mazarrasa, I., Neto, J. M., Bouma, T. J., Grandjean, T., Garcia-Orellana, J., Masque, P., Recio, M., Serrano, O., Puente, A., and Juanes, J. A.: Drivers of variability in Blue Carbon stocks and burial rates across European estuarine habitats, Science of the Total Environment 886, 163957, 10.1016/j.scitotenv.2023.163957, 2023.

Mazarrasa, I., Lavery, P., Duarte, C. M., Lafratta, A., Lovelock, C. E., Macreadie, P. I., Samper-Villarreal, J., Salinas, C., Sanders, C. J., Trevathan-Tackett, S., Young, M., Steven, A., and Serrano, O.: Factors Determining Seagrass Blue Carbon Across Bioregions and Geomorphologies, Global Biogeochemical Cycles, 35, 10.1029/2021gb006935, 2021.

McKenzie, L. J., Yaakub, S. M., and Yoshida, R. L.: Seagrass habitats of Singapore: environmental drivers and key processes, Raffles Bulletin of Zoology, 2016.

Meteorological Service Singapore: 2024 Annual Climate Assessment Report, Meteorological Service Singapore, 2024.

Miyajima, T., Hori, M., Hamaguchi, M., Shimabukuro, H., Adachi, H., Yamano, H., and Nakaoka, M.: Geographic variability in organic carbon stock and accumulation rate in sediments of East and Southeast Asian seagrass meadows, Global Biogeochemical Cycles, 29, 397–415, 10.1002/2014gb004979, 2015.

Ndhlovu, A., Adams, J. B., and Von der Heyden, S.: Large-scale environmental signals in seagrass blue carbon stocks are hidden by high variability at local scales, Science of the Total Environment, 921, 170917, 10.1016/j.scitotenv.2024.170917, 2024.

Neubauer, S. C. and Megonigal, J. P.: Moving beyond global warming potentials to quantify the climatic role of ecosystems, Ecosystems, 18, 1000–1013, 2015.

Orphan, V. J., Hinrichs, K.-U., Ussler III, W., Paull, C. K., Taylor, L., Sylva, S. P., Hayes, J. M., and DeLong, E. F.: Comparative analysis of methane-oxidizing archaea and sulfate-reducing bacteria in anoxic marine sediments, Applied and Environmental Microbiology, 67, 1922–1934, 2001.

Phang, V. X. H., Chou, L. M., and Friess, D. A.: Ecosystem carbon stocks across a tropical intertidal habitat mosaic of mangrove forest, seagrass meadow, mudflat and sandbar, Earth Surface Processes and Landforms, 40, 1387–1400, 10.1002/esp.3745, 2015.

R Core Team: R: A Language and Environment for Statistical Computing, R Foundation for Statistical Computing, Vienna, Austria, 2026.

Reeburgh, W. S.: Oceanic methane biogeochemistry, Chemical reviews, 107, 486–513, 2007.

Ricart, A. M., York, P. H., Bryant, C. V., Rasheed, M. A., Ierodiaconou, D., and Macreadie, P. I.: High variability of Blue Carbon storage in seagrass meadows at the estuary scale, Scientific Reports, 10, 5865, 2020.

Rodriguez, K., Ricci, F., Ni, G., Iram, N., Palfreyman, R., Gonzalez-Garcia, R. A., Heffernan, J., Greening, C., Adame, M. F., and Marcellin, E.: Abundant and active acetogens enhance the carbon dioxide sink of Blue Carbon ecosystems, Microbiome, 13, 207, 10.1186/s40168-025-02209-4, 2025.

Rosentreter, J. A., Al-Haj, A. N., Fulweiler, R. W., and Williamson, P.: Methane and Nitrous Oxide Emissions Complicate Coastal Blue Carbon Assessments, Global Biogeochemical Cycles, 35, 10.1029/2020GB006858, 2021.

Ruiz-Fernández, A. C., Sanchez-Cabeza, J.-A., Cuéllar-Martínez, T., Pérez-Bernal, L. H., Carnero-Bravo, V., Ávila, E., and Cardoso-Mohedano, J. G.: Increasing salinization and organic carbon burial rates in seagrass meadows from an anthropogenically-modified coastal lagoon in southern Gulf of Mexico, Estuarine, Coastal and Shelf Science, 242, 10.1016/j.ecss.2020.106843, 2020.

Serrano, O., Lavery, P. S., Duarte, C. M., Kendrick, G. A., Calafat, A., York, P. H., Steven, A., and Macreadie, P. I.: Can mud (silt and clay) concentration be used to predict soil organic carbon content within seagrass ecosystems?, Biogeosciences, 13, 4915–4926, 10.5194/bg-13-4915-2016, 2016.

Serrano, O., Lovelock, C. E., B. Atwood, T., Macreadie, P. I., Canto, R., Phinn, S., Arias-Ortiz, A., Bai, L., Baldock, J., Bedulli, C., Carnell, P., Connolly, R. M., Donaldson, P., Esteban, A., Ewers Lewis, C. J., Eyre, B. D., Hayes, M. A., Horwitz, P., Hutley, L. B., Kavazos, C. R. J., Kelleway, J. J., Kendrick, G. A., Kilminster, K., Lafratta, A., Lee, S., Lavery, P. S., Maher, D. T., Marbà, N., Masque, P., Mateo, M. A., Mount, R., Ralph, P. J., Roelfsema, C., Rozaimi, M., Ruhon, R., Salinas, C., Samper-Villarreal, J., Sanderman, J., J. Sanders, C., Santos, I., Sharples, C., Steven, A. D. L., Cannard, T., Trevathan-Tackett, S. M., and Duarte, C. M.: Australian vegetated coastal ecosystems as global hotspots for climate change mitigation, Nature Communications, 10, 10.1038/s41467-019-12176-8, 2019.

Stankovic, M., Mishra, A. K., Rahayu, Y. P., Lefcheck, J., Murdiyarso, D., Friess, D. A., Corkalo, M., Vukovic, T., Vanderklift, M. A., Farooq, S. H., Gaitan-Espitia, J. D., and Prathep, A.: Blue carbon assessments of seagrass and mangrove ecosystems in South and Southeast Asia: Current progress and knowledge gaps, Science of the Total Environment 904, 166618, 10.1016/j.scitotenv.2023.166618, 2023.

Stankovic, M., Ambo-Rappe, R., Carly, F., Dangan-Galon, F., Fortes, M. D., Hossain, M. S., Kiswara, W., Van Luong, C., Minh-Thu, P., Mishra, A. K., Noiraksar, T., Nurdin, N., Panyawai, J., Rattanachot, E., Rozaimi, M., Soe Htun, U., and Prathep,

A.: Quantification of blue carbon in seagrass ecosystems of Southeast Asia and their potential for climate change mitigation, Sci Total Environ, 783, 146858, 10.1016/j.scitotenv.2021.146858, 2021.
Tan, Y. H. J., Tham, J. K. Q., Paul, A., Rana, U., Ang, H. P., Nguyen, N. T. H., Yee, A. T. K., Leong, B. P. I., Drummond, S., and Tun, K. P. P.: Remote sensing mapping of the regeneration of coastal natural habitats in Singapore: Implications for marine conservation in tropical cities, Singapore Journal of Tropical Geography, 44, 130–148, 10.1111/sjtg.12454, 2022.
Twilley, R. R., Rovai, A. S., and Riul, P.: Coastal morphology explains global blue carbon distributions
Frontiers in Ecology and the Environment, 16, 503–508, 10.1002/fee.1937, 2018.
Unsworth, R. K. F., Cullen-Unsworth, L. C., Jones, B. L. H., and Lilley, R. J.: The planetary role of seagrass conservation, Science, 377, 609–613, doi:10.1126/science.abq6923, 2022.
Williamson, P., Gattuso, J.-P., and Pearce, C. R.: Carbon Removal Using Coastal Blue Carbon Ecosystems Is Uncertain and Unreliable , With Questionable Climatic Cost-Effectiveness, Frontiers in Climate, 4, 1–14, 10.3389/fclim.2022.853666, 2022.
York, P. H., Macreadie, P. I., and Rasheed, M. A.: Blue Carbon stocks of Great Barrier Reef deep-water seagrasses, Biology Letters, 14, 20180529, 10.1098/rsbl.2018.0529, 2018.
Zheng, P., Chen, G., Lan, W., Li, S., Li, M., Chen, S., An, W., Chen, J., Yu, S., and Chen, B.: Determining effect of seagrass-mediated CO2 flux on the atmospheric cooling potential of a subtropical intertidal seagrass meadow, Marine Pollution Bulletin, 188, 114676, 10.1016/j.marpolbul.2023.114676, 2023.